NASA/TM-2006-214285

A Micromechanics-Based Damage Model for $[\pm\theta/90_n]_s$ Composite Laminates

Joan-Andreu Mayugo
Escola Politècnica Superior, Universitat de Girona, Girona, Spain

Pedro P. Camanho
Faculdade de Engenharia, Universidade do Porto, Porto, Portugal

Pere Maimí
Escola Politècnica Superior, Universitat de Girona, Girona, Spain

Carlos G. Dávila
Langley Research Center, Hampton, Virginia

March 2006

The NASA STI Program Office . . . in Profile

Since its founding, NASA has been dedicated to the advancement of aeronautics and space science. The NASA Scientific and Technical Information (STI) Program Office plays a key part in helping NASA maintain this important role.

The NASA STI Program Office is operated by Langley Research Center, the lead center for NASA's scientific and technical information. The NASA STI Program Office provides access to the NASA STI Database, the largest collection of aeronautical and space science STI in the world. The Program Office is also NASA's institutional mechanism for disseminating the results of its research and development activities. These results are published by NASA in the NASA STI Report Series, which includes the following report types:

- TECHNICAL PUBLICATION. Reports of completed research or a major significant phase of research that present the results of NASA programs and include extensive data or theoretical analysis. Includes compilations of significant scientific and technical data and information deemed to be of continuing reference value. NASA counterpart of peer-reviewed formal professional papers, but having less stringent limitations on manuscript length and extent of graphic presentations.

- TECHNICAL MEMORANDUM. Scientific and technical findings that are preliminary or of specialized interest, e.g., quick release reports, working papers, and bibliographies that contain minimal annotation. Does not contain extensive analysis.

- CONTRACTOR REPORT. Scientific and technical findings by NASA-sponsored contractors and grantees.

- CONFERENCE PUBLICATION. Collected papers from scientific and technical conferences, symposia, seminars, or other meetings sponsored or co-sponsored by NASA.

- SPECIAL PUBLICATION. Scientific, technical, or historical information from NASA programs, projects, and missions, often concerned with subjects having substantial public interest.

- TECHNICAL TRANSLATION. English-language translations of foreign scientific and technical material pertinent to NASA's mission.

Specialized services that complement the STI Program Office's diverse offerings include creating custom thesauri, building customized databases, organizing and publishing research results ... even providing videos.

For more information about the NASA STI Program Office, see the following:

- Access the NASA STI Program Home Page at ***http://www.sti.nasa.gov***

- E-mail your question via the Internet to help@sti.nasa.gov

- Fax your question to the NASA STI Help Desk at (301) 621-0134

- Phone the NASA STI Help Desk at (301) 621-0390

- Write to:
  NASA STI Help Desk
  NASA Center for AeroSpace Information
  7121 Standard Drive
  Hanover, MD 21076-1320

NASA/TM-2006-214285

A Micromechanics-Based Damage Model for $[\pm\theta/90_n]_s$ Composite Laminates

Joan-Andreu Mayugo
Escola Politècnica Superior, Universitat de Girona, Girona, Spain

Pedro P. Camanho
Faculdade de Engenharia, Universidade do Porto, Porto, Portugal

Pere Maimí
Escola Politècnica Superior, Universitat de Girona, Girona, Spain

Carlos G. Dávila
Langley Research Center, Hampton, Virginia

National Aeronautics and
Space Administration

Langley Research Center
Hampton, Virginia 23681-2199

March 2006

Available from:

NASA Center for AeroSpace Information (CASI)
7121 Standard Drive
Hanover, MD 21076-1320
(301) 621-0390

National Technical Information Service (NTIS)
5285 Port Royal Road
Springfield, VA 22161-2171
(703) 605-6000

A micromechanics-based damage model for $[\pm\theta/90_n]_s$ composite laminates

J.A. Mayugo [a], P.P. Camanho [b], P. Maimí [a], C.G. Dávila [c]

[a] *AMADE, Escola Politècnica Superior, Universitat de Girona, Campus Montilivi, 17071 Girona, Spain*

[b] *DEMEGI, Faculdade de Engenharia, Universidade do Porto, Rua Dr. Roberto Frias, 4200-465, Porto, Portugal*

[c] *NASA Langley Research Center, Hampton, Virginia, U.S.A.*

Abstract

A new damage model based on a micromechanical analysis of cracked $[\pm\theta/90_n]_s$ laminates subjected to multiaxial loads is proposed. The model predicts the onset and accumulation of transverse matrix cracks in uniformly stressed laminates, the effect of matrix cracks on the stiffness of the laminate, as well as the ultimate failure of the laminate. The model also accounts for the effect of the ply thickness on the ply strength. Predictions relating the elastic properties of several laminates and multiaxial loads are presented.

Key words: Failure criteria, Micromechanics, Damage Mechanics.

1 Introduction

The aerospace industry is committed to improve the performance of aircraft whilst reducing emissions and weight. Such a goal can be achieved by the use of advanced polymer-based composite materials, that have excellent properties for aerospace applications, such as low density, and fatigue and corrosion resistance.

The design procedure used for advanced composite structures relies on a 'building-block' approach [1], where a large number of experimental tests are performed throughout the product development process. The use of improved analytical or numerical models in the prediction of the mechanical behavior of composite structures can significantly reduce the cost of such structures. Such models should predict the onset of material degradation, the effect of the

non-critical damage mechanisms on the stiffness of the laminate, and ultimate structural failure.

Strength-based failure criteria are commonly used to predict failure in composite materials [2]-[7]. Failure criteria predict the onset of the several damage mechanisms occurring in composites and, depending on the laminate, geometry and loading conditions, may also predict structural collapse.

In multidirectional composite laminates, damage accumulates during the loading process. Final failure occurs as a result of damage accumulation and stress re-distribution. The ultimate failure load is higher than the initial damage predicted by strength-based failure criteria. Furthermore, stress- or strain-based failure criteria cannot represent size effects that occur in quasi-brittle materials [8].

Simplified models, such as the ply discount method where some scalar components of the stiffness tensor are reduced to approximately zero when damage is predicted, are often used by the industry to predict ultimate laminate failure. However, these methods cannot represent with satisfactory accuracy the progressive reduction of the stiffness of a laminate as a result of the accumulation of matrix cracks.

Constitutive laws based on Continuum Damage Mechanics (CDM) have been proposed to predict the material response, from the onset of damage up to final collapse [9]-[14]. Although the existing CDM models can accurately predict the evolution of damage, they usually rely on fitting parameters that need to be measured at laminate level, such as the critical values of thermodynamic forces [14].

Three-dimensional models based on CDM use material properties measured at ply level. Damage mechanisms such as transverse matrix cracks are represented by strain-softening constitutive models and bands of localized deformation. The implementation of strain-softening models in finite element models may cause convergence difficulties during the iterative solution procedure. Furthermore, strain-softening models require regularization techniques to provide mesh-independent solutions [15,16].

Alternative methods based on the combination of elastic analysis of cracked plies and finite Fracture Mechanics provide the basis for an accurate representation of the response of composite materials [17]-[30]. Micromechanical models have been developed to predict the initiation and evolution of transverse matrix cracks under either in-plane shear or transverse tension. Generalizations of these models are required for the more usual case of multiaxial loading.

In order to predict ultimate failure, a micromechanical model needs to be used in combination with a fiber failure criterion. Furthermore, a general methodology to predict laminate strength should be able to predict matrix cracking under high values of transverse compression. These damage mechanisms usually correspond to the final failure of laminates under uniform states of stress [6].

The objective of this work is to define a new damage model based on micromechanical models of transverse matrix cracks to predict the onset and evolution of transverse matrix cracks under multiaxial loading. A new constitutive model is derived based on the thermodynamics of irreversible processes. Continuum Damage Mechanics provides a rigorous framework to define the constitutive model and to develop the corresponding computational implementation. The model proposed herein represents transverse matrix cracks as distributed damage and does not require any regularization to yield mesh-independent results when implemented in finite element models. Furthermore, the model is able to predict the onset and propagation of matrix transverse cracks under multiaxial loading as well as the final failure of uniformly stressed laminates where a periodic distribution of transverse matrix cracks can be assumed.

2 Micromechanical model of transverse matrix cracks under multiaxial loading

The proposed continuum damage model is based on two major components: a set of stress based failure criteria and a micromechanical model of transverse matrix cracking in multidirectional laminates.

The failure criteria define the onset of transverse matrix cracking, i.e. the activation of the damage variables. A micromechanical model of transverse matrix cracks is required to define the evolution of the damage variables.

Several micromechanical models of transverse matrix cracks that have been proposed in the literature [19,30] can be used within the framework developed here. The micromechanical model proposed by Tan and Nuismer [17,18] accounts for the effects of the adjoining plies on the homogenized elastic properties of a cracked ply. This micromechanical model is the basis of the developments presented in this work. The models are considered as micromechanical in the sense that they are based on a boundary value problem that explicitly represents transverse matrix cracks. However, the fibers and the matrix are not represented explicitly.

Using the assumption of generalized plane strain, Tan and Nuismer [17,18] developed a model able to relate the density of transverse matrix cracks in a central 90º ply to the homogenized elastic properties of that ply. The model developed by Tan and Nuismer was used for the prediction of the evolution of transverse matrix cracks under either in-plane shear or transverse tensile stresses.

The laminates under investigation are symmetric and balanced with a $[\pm\theta/90_{\mathrm{n}}]_s$ layup containing a periodic distribution of transverse matrix cracks, as shown in Figure 1. The micromechanical analysis of a balanced symmetrical laminate requires the division of the laminate in two sub-laminates: the 90° layers in the middle layer (sublaminate 1), and the outer plies (sublaminate 2).

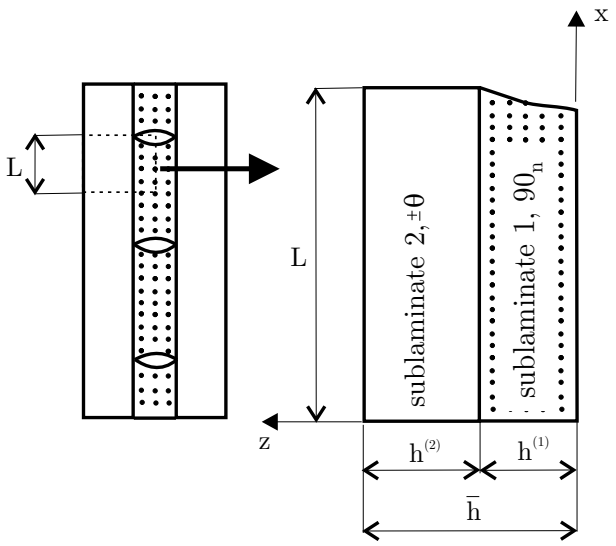

Fig. 1. One-quarter of the laminate.

Sublaminate 1 is taken as transversely isotropic. The outer layers, sublaminate 2, may contain several layers with different fiber orientations but must be orthotropic in the laminate global system (x, y and z coordinates). The expressions for the compliance and stiffness tensors for the laminate, sublaminate 1, and sublaminate 2 are shown in Appendix A. In what follows, the superscripts (1) and (2) corresponds to the sublaminate 1 and 2, respectively.

2.1 Damage dependent constitutive tensor

The stiffness tensor $\bar{\mathbf{A}}$ of the balanced and symmetric laminate shown in Figure 1 can be written as a function of one-half of the distance between transverse matrix cracks (L) in sublaminate 1:

$$\bar{\mathbf{A}}(L) = \begin{bmatrix} \bar{A}(L)_{11} & \bar{A}(L)_{12} & 0 \\ \bar{A}(L)_{21} & \bar{A}(L)_{22} & 0 \\ 0 & 0 & \bar{A}(L)_{66} \end{bmatrix} \tag{1}$$

where the terms $\bar{A}_{ij}(L), i, j = 1, 2, 6$ are obtained from the Tan and Nuismer model [18] which is summarized in Appendix A.

The undamaged stiffness matrix $\bar{\mathbf{Q}}$ of the laminate is obtained from lamination theory using the undamaged stiffness matrix of sublaminate 1, $\bar{\mathbf{Q}}^{(1)}$, and the stiffness matrix of sublaminate 2, $\bar{\mathbf{Q}}^{(2)}$. Therefore,

$$Q_{ij}^{(1)} = \frac{1}{h^{(1)}} \left(\bar{h}\bar{Q}_{ij} - h^{(2)} Q_{ij}^{(2)} \right) \tag{2}$$

where $\bar{h} = h^{(1)} + h^{(2)}$.

Assuming that the degradation due to the transverse matrix cracks only occur in sublaminate 1, the damaged stiffness tensor of laminate 1 is given as:

$$\bar{A}_{ij}^{(1)}(L) = \frac{1}{h^{(1)}} \left(\bar{h}\bar{A}_{ij}(L) - h^{(2)} Q_{ij}^{(2)} \right) \tag{3}$$

where $\bar{A}_{ij}^{(1)}(L)$ $(i, j = 1, 2, 6)$ are the scalar components of the stiffness tensor of sublaminate 1. These components are a function of the distance between transverse matrix cracks (L, defined in Figure 1).

Having defined $\bar{A}_{ij}^{(1)}(L)$, it is possible to calculate the effective transverse modulus, Poisson ratio, and shear modulus of the 90° ply:

$$\bar{E}_2^{(1)}(L) = \bar{E}_x^{(1)}(L) = \bar{A}_{11}^{(1)}(L) - \frac{\left[\bar{A}_{12}^{(1)}(L)\right]^2}{\bar{A}_{22}^{(1)}(L)} \tag{4}$$

$$\bar{v}_{21}^{(1)}(L) = \bar{v}_{xy}^{(1)}(L) = \frac{\bar{A}_{12}^{(1)}(L)}{\bar{A}_{22}^{(1)}(L)} \tag{5}$$

$$\bar{G}_{12}^{(1)}(L) = \bar{G}_{xy}^{(1)}(L) = \bar{A}_{66}^{(1)}(L) \tag{6}$$

One noticeable feature of this model is that the degradation of the transverse modulus is equal to the degradation of the minor Poisson ratio:

$$\frac{\bar{\upsilon}_{21}^{(1)}(L)}{\bar{E}_{2}^{(1)}(L)} = \frac{\upsilon_{21}}{E_2} \tag{7}$$

Therefore, the quotient υ_{21}/E_2 is not a function of damage. This observation is in agreement with several other models, such as the ones proposed by Laws et al. [23,24], and Nguyen [25].

From equation (7) it can be concluded that the plane stress compliance tensor of the damaged sublaminate 1, $\mathbf{H}^{(1)}$, only contains two components that depend on the density of transverse matrix cracks: $H_{22}^{(1)}(L)$ and $H_{66}^{(1)}(L)$. The tensor $\mathbf{H}^{(1)}$, is established as a function of the spacing of transverse matrix cracks, L, as:

$$\mathbf{H}^{(1)} = \begin{bmatrix} \dfrac{1}{E_1} & -\dfrac{\upsilon_{21}}{E_2} & 0 \\ -\dfrac{\upsilon_{12}}{E_1} & H_{22}^{(1)}(L) & 0 \\ 0 & 0 & H_{66}^{(1)}(L) \end{bmatrix} \tag{8}$$

where:

$$H_{22}^{(1)}(L) = \frac{1}{\bar{E}_{2}^{(1)}(L)} = \frac{\bar{A}_{22}^{(1)}(L)}{\bar{A}_{11}^{(1)}(L)\bar{A}_{22}^{(1)}(L) - \left[\bar{A}_{12}^{(1)}(L)\right]^2} \tag{9}$$

$$H_{66}^{(1)}(L) = \frac{1}{\bar{G}_{12}^{(1)}(L)} = \frac{1}{\bar{A}_{66}^{(1)}(L)} \tag{10}$$

The evolution of the laminate stiffness as a function of the density crack $\beta = 1/(2L)$ is shown in Figure 2 for a $[\pm 25/90_3]_s$ laminate with the material properties shown in Table 1. The relation between the homogenized elastic properties of the cracked ply (sublaminate 1) and β is shown in Figure 3.

Table 1
Elastic properties of typical carbon/epoxy composite.

E_1 (GPa)	E_2 (GPa)	G_{12} (GPa)	υ_{12}
163.4	11.9	6.2	0.30

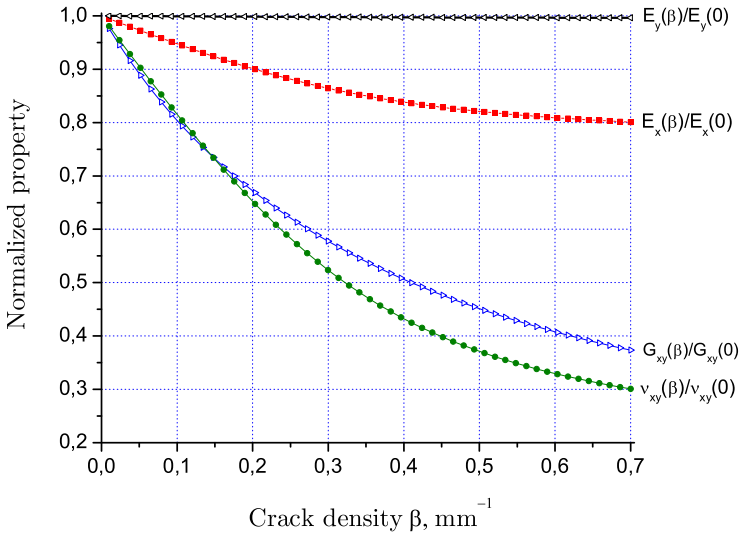

Fig. 2. Laminate stiffness as a function of the matrix crack density in the 90° ply.

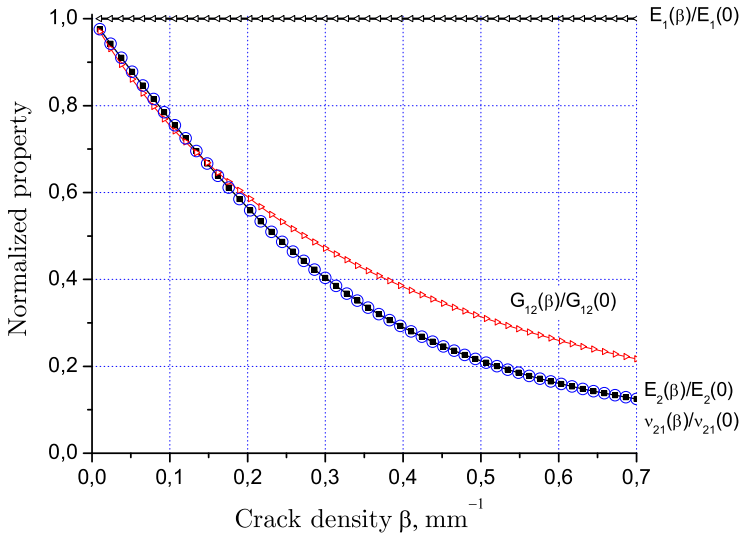

Fig. 3. Effective elastic properties of the 90° ply as a function of the matrix crack density.

Figures 2 and 3 show that the Young modulus of the laminate, E_x, and the Young modulus of sublaminate 1, E_1, are not affected by the presence of transverse matrix cracks. Furthermore, the curves $E_2(\beta)/E_2$ and $\upsilon_{21}(\beta)/\upsilon_{21}$ are coincident (Figure 3), as a result of equation (7).

2.2 Onset of matrix transverse cracks under multiaxial loading

The onset of transverse matrix cracking in a ply under the combined effect of in-plane shear stresses and transverse tensile stresses needs to be predicted using an appropriate failure criterion. The failure criterion should be established in terms of the actual strengths of a ply when it is embedded in a multidirectional laminate (in-situ strengths).

2.2.1 In-situ strengths

A methodology to predict the onset of matrix transverse cracking must be able to predict the in-situ strengths of a ply. Both the transverse tensile and in-plane shear strengths of a ply embedded in a multidirectional laminate are higher that the corresponding values measured in unidirectional laminates [31].

Models based on elastic analysis of the cracked laminate shown in Figure 1 have been proposed to predict the in-situ strengths. Such an approach is only appropriate for the strength prediction of thin embedded plies. For a thin ply, it can be assumed that the defects at the micromechanical level can be represented as cracks that have a length equal to the ply thickness and can only propagate in the direction of the fibers [32].

However, for a thick ply the length of the 'effective crack' is smaller than the ply thickness and propagates in a first phase along the thickness direction [32]. Therefore, a methodology to predict the onset of matrix transverse cracking based on the cracked ply model represented in Figure 1 is not appropriate for thick plies.

Instead, the thick ply model described in [32] is used. The tensile transverse in-situ strengths of sublaminate (1) is [32]:

$$\text{For a thin embedded ply: } Y_{\mathrm{T}} = \sqrt{\frac{8G_{\mathrm{Ic}}}{\pi t \Lambda_{22}^{o}}} \tag{11}$$

$$\text{For a thick ply: } Y_{\mathrm{T}} = 1.12\sqrt{2}Y_{\mathrm{T}}^{\mathrm{ud}} \tag{12}$$

where $Y_{\mathrm{T}}^{\mathrm{ud}}$ is the tensile transverse strength measured in a unidirectional test specimen, t is the thickness of sublaminate 1, G_{Ic} is the mode I intralaminar fracture toughness, and Λ_{22}° is defined as:

$$\Lambda_{22}^{\circ} = 2\left(\frac{1}{E_2} - \frac{\upsilon_{21}^2}{E_1}\right) \tag{13}$$

The in-situ shear strengths are obtained as [31]:

$$S_{\mathrm{L}} = \sqrt{\frac{\left(1 + \chi\phi G_{12}^2\right)^{1/2} - 1}{3\chi G_{12}}} \tag{14}$$

where χ is the shear response factor defined in [31], and the parameter ϕ is calculated according to the configuration of the ply:

$$\text{For a thick ply:} \quad \phi = \frac{12\left(S_L^{\mathrm{ud}}\right)^2}{G_{12}} + 18\chi\left(S_L^{\mathrm{ud}}\right)^4 \tag{15}$$

$$\text{For a thin ply:} \quad \phi = \frac{48 G_{\mathrm{IIc}}}{\pi t} \tag{16}$$

where S_L^{ud} is the shear strength measured using an unidirectional test specimen and G_{IIc} is the mode II fracture toughness.

2.2.2 Failure criterion for the prediction of transverse cracking under multiaxial loading

In general, a ply represented by sublaminate 1 in Figure 1 is subjected to transverse tensile stresses and in-plane shear stresses. Under pure in-plane shear or pure transverse tension, the onset of transverse matrix cracking is predicted by comparing the components of the stress tensor with the respective in-situ strengths (defined in the previous section).

Under multiaxial loading, it is necessary to use a failure criterion to predict the onset of matrix cracking. The LaRC04 [4,5] failure criteria are a function of the components of the stress tensor and in-situ strengths. For transverse tension, the criterion used is:

$$(1-g)\frac{\sigma_{22}}{Y_{\mathrm{T}}} + g\left(\frac{\sigma_{22}}{Y_{\mathrm{T}}}\right)^2 + \left(\frac{\sigma_{12}}{S_{\mathrm{L}}}\right)^2 - 1 \leq 0 \text{ with } \sigma_{22} \geq 0 \tag{17}$$

where $g = G_{\mathrm{Ic}}/G_{\mathrm{IIc}}$. G_{IIc} is the mode II component of the fracture toughness associated with matrix transverse cracking.

Under moderate values of transverse compression, the crack plane is parallel to the laminate thickness direction. The LaRC04 failure criterion is:

$$\frac{1}{S_L}\left\langle |\sigma_{12}| + \eta^L \sigma_{22} \right\rangle - 1 \leq 0 \text{ with } \sigma_{22} < 0 \tag{18}$$

where η^L is the coefficient of longitudinal influence defined in [4,5].

2.3 Evolution of matrix transverse cracks under multiaxial loading

To predict laminate failure under general loading, it is necessary to know how the density of transverse matrix cracks evolves in a ply subjected to combined in-plane shear and transverse tensile stresses. The evolution law is derived from the micromechanical model presented in this section.

To define the damage evolution law, it is necessary to relate the applied stress or strain state to the density of transverse matrix cracks. This relation is obtained from a Fracture Mechanics analysis of cracked plies combined with the definition of the damaged constitutive tensor.

2.3.1 Transverse tension

Tan and Nuismer [18] obtained a closed-form expression that defines the evolution of transverse matrix cracks under uniaxial stress states (either transverse tension or in-plane shear).

To predict failure under multiaxial loading, i.e. when the lamina is simultaneously under tensile and in-plane shear strains, ε_{xx} and γ_{xy} respectively, it is necessary to derive a relation between the density of transverse matrix cracks and the applied multiaxial strain state. It is assumed that the relation between the tensile and shear strains is constant throughout the loading history:

$$\kappa = \frac{\gamma_{xy}}{\varepsilon_{xx}} \text{ with } \varepsilon_{xx} > 0 \tag{19}$$

where κ is the *multiaxial strain ratio*.

Consider a ply with crack spacing L, as shown in Figure 4 a).

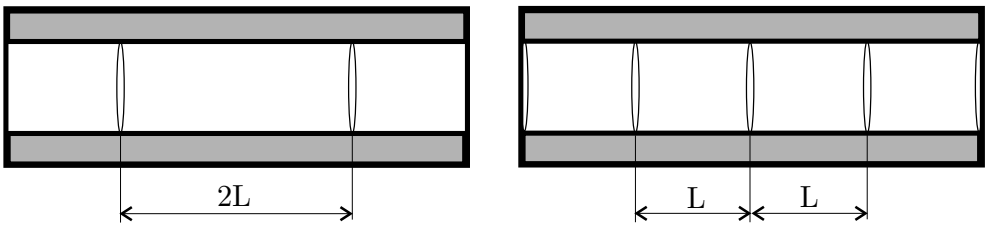

a) Crack spacing 2L b) Crack spacing L

Fig. 4. Progression of transverse matrix cracks.

The strain energy in a laminate cell of length $2L$ subjected to transverse tension and in-plane shear just prior to fracture, U_{2L}, can be established as a function of the strain tensor and of the crack spacing as:

$$U_{2L} = 2\overline{h}Lb\left[E_x(L)\varepsilon_{xx}^2 + A_{66}(L)\gamma_{xy}^2\right] \tag{20}$$

where $E_x(L)$ is the axial stiffness of the laminate with a crack spacing of $2L$ and b is the specimen width; $A_{66}(L)$ is the laminate effective shear stiffness corresponding to a crack spacing of $2L$, $2\overline{h}$ and $2L$ are the laminate thickness and the distance between two consecutive transverse matrix cracks, respectively.

After the propagation of transverse matrix cracks, Figure 4 b), the strain energy in the original unit cell of length $2L$ is:

$$U_L = 2\overline{h}Lb\left[E_x\left(\frac{L}{2}\right)\varepsilon_{xx}^2 + A_{66}\left(\frac{L}{2}\right)\gamma_{xy}^2\right] \tag{21}$$

where $E_x(L/2)$ and $A_{66}(L/2)$ are respectively the axial stiffness and the laminate effective shear stiffness corresponding to a crack density defined by L.

The energy required to generate a new matrix crack in a ply equals the loss of strain energy of the laminate [18]. Therefore the difference between equation (20) and equation (21) is equal to the energy released by the sublaminate 1:

$$\begin{aligned}\Delta U &= U_{2L} - U_L = \\ &= 2\overline{h}Lb\left\{\left[E_x(L) - E_x\left(\frac{L}{2}\right)\right]\varepsilon_{xx}^2 + \left[A_{66}(L) - A_{66}\left(\frac{L}{2}\right)\right]\gamma_{xy}^2\right\}\end{aligned} \tag{22}$$

or:

$$\Delta U = 2h^{(1)}bG_c = 2h^{(1)}bG_I + 2h^{(1)}bG_{II} \tag{23}$$

where G_c is the mixed-mode fracture toughness of sublaminate 1 under tensile (mode I) and shear (mode II) loading. From (22) and (23):

$$\left[E_x(L) - E_x\left(\frac{L}{2}\right)\right]\varepsilon_{xx}^2 + \left[A_{66}(L) - A_{66}\left(\frac{L}{2}\right)\right]\gamma_{xy}^2 = \frac{h^{(1)}G_c}{\overline{h}L} \tag{24}$$

Using the definition of κ given in (19), equation (24) can be re-written as a function of the strains:

$$\left\{\left(E_x(L) - E_x\left(\frac{L}{2}\right)\right) + \kappa^2\left[A_{66}(L) - A_{66}\left(\frac{L}{2}\right)\right]\right\}\varepsilon_{xx}^2 = \frac{h^{(1)}G_c}{\overline{h}L} \tag{25}$$

or:

$$\left\{\frac{1}{\kappa^2}\left[E_x(L) - E_x\left(\frac{L}{2}\right)\right] + \left[A_{66}(L) - A_{66}\left(\frac{L}{2}\right)\right]\right\}\gamma_{xy}^2 = \frac{h^{(1)}G_c}{\overline{h}L} \tag{26}$$

The relations between normal and shear strains, and the crack density are obtained as:

$$\varepsilon_{xx} = \sqrt{\frac{h^{(1)}G_c}{\overline{h}L}\frac{1}{\left[E_x(L) - E_x\left(\frac{L}{2}\right)\right] + \kappa^2\left[A_{66}(L) - A_{66}\left(\frac{L}{2}\right)\right]}} \tag{27}$$

$$\gamma_{xy} = \sqrt{\frac{h^{(1)}G_c}{\overline{h}L}\frac{\kappa^2}{\left[E_x(L) - E_x\left(\frac{L}{2}\right)\right] + \kappa^2\left[A_{66}(L) - A_{66}\left(\frac{L}{2}\right)\right]}} = \kappa\varepsilon_{xx} \tag{28}$$

Equations (27) and (28), are established as a function of the mixed-mode fracture toughness G_c that needs to be defined.

The mixed-mode fracture toughness is defined in terms of the mode I and mode II components as:

$$G_c = G_{\mathrm{I}} + G_{\mathrm{II}} \tag{29}$$

From (29) and (24):

$$\frac{h^{(1)}G_c}{\overline{h}L} = \frac{h^{(1)}G_{\mathrm{I}}}{\overline{h}L} + \frac{h^{(1)}G_{\mathrm{II}}}{\overline{h}L} = \tag{30}$$

$$= \left[E_x(L) - E_x\left(\frac{L}{2}\right)\right]\varepsilon_{xx}^2 + \left[A_{66}(L) - A_{66}\left(\frac{L}{2}\right)\right]\gamma_{xy}^2 \tag{31}$$

and:

$$\frac{h^{(1)}G_{\mathrm{I}}}{\overline{h}L} = \left[E_x(L) - E_x\left(\frac{L}{2}\right)\right]\varepsilon_{xx}^2 \tag{32}$$

$$\frac{h^{(1)}G_{\mathrm{II}}}{\overline{h}L} = \left[A_{66}(L) - A_{66}\left(\frac{L}{2}\right)\right]\gamma_{xy}^2 \tag{33}$$

Dividing equations (32) and (33) by (25) and (26) respectively:

$$A_I = \frac{G_{\mathrm{I}}}{G_c} = \frac{\left[E_x(L) - E_x\left(\frac{L}{2}\right)\right]}{\left[E_x(L) - E_x\left(\frac{L}{2}\right)\right] + \kappa^2\left[A_{66}(L) - A_{66}\left(\frac{L}{2}\right)\right]} \tag{34}$$

$$A_{II} = \frac{G_{\mathrm{II}}}{G_c} = \frac{\kappa^2\left[A_{66}(L) - A_{66}\left(\frac{L}{2}\right)\right]}{\left[E_x(L) - E_x\left(\frac{L}{2}\right)\right] + \kappa^2\left[A_{66}(L) - A_{66}\left(\frac{L}{2}\right)\right]} \tag{35}$$

A_I and A_{II} are the ratios between the mode I and mode II components of the energy release rate and the mixed-mode fracture toughness; A_I and A_{II} can be obtained as a function of the crack density and of the multiaxial strain ratio κ.

Taking into account that the energy release rate under mixed-mode loading is the sum of the mode I and mode II energy release rates, equation (29) can be established as:

$$1 = \frac{G_{\mathrm{I}}}{G_c} + \frac{G_{\mathrm{II}}}{G_c} \tag{36}$$

$$1 = A_I + A_{II} \tag{37}$$

The criterion proposed by Hahn [33] for the prediction of transverse matrix cracking under transverse tensile and in-plane shear loads is used:

$$(1-g)\sqrt{\frac{G_{\mathrm{IIc}}}{G_{\mathrm{Ic}}}} + g\frac{G_{\mathrm{I}}}{G_{\mathrm{Ic}}} + \frac{G_{\mathrm{II}}}{G_{\mathrm{IIc}}} = 1 \tag{38}$$

Substituting equations (34) and (35) into (38) gives:

$$(1-g)\sqrt{\frac{A_I G_c}{G_{\mathrm{Ic}}}} + g\frac{A_I G_c}{G_{\mathrm{Ic}}} + \frac{A_{II} G_c}{G_{\mathrm{IIc}}} = 1 \tag{39}$$

or:

$$(1-g)\sqrt{\frac{A_I G_c}{G_{\mathrm{Ic}}}} + g\frac{A_I G_c}{G_{\mathrm{Ic}}} + \frac{(1-A_I)\, G_c}{G_{\mathrm{IIc}}} = 1 \tag{40}$$

The positive real solution of (40) is:

$$G_c = G_{\mathrm{IIc}} + \frac{A_I}{2}\frac{(G_{\mathrm{Ic}} - G_{\mathrm{IIc}})^2}{G_{\mathrm{Ic}}}\left(1 - \sqrt{1 + \frac{4}{A_I}\frac{G_{\mathrm{Ic}} G_{\mathrm{IIc}}}{(G_{\mathrm{Ic}} - G_{\mathrm{IIc}})^2}}\right) \tag{41}$$

where A_I, which is given by equations (34), depends on the density of transverse matrix cracks, β, and on the multiaxial strain ratio, κ (equation (19)).

Figures 5 and 6 show respectively the relation between the crack density β and ε_{xx} and γ_{xy} for different multiaxial strain ratios. A $[\pm 25/90_3]_s$ laminate with the elastic properties shown in Table 1 is used in the predictions.

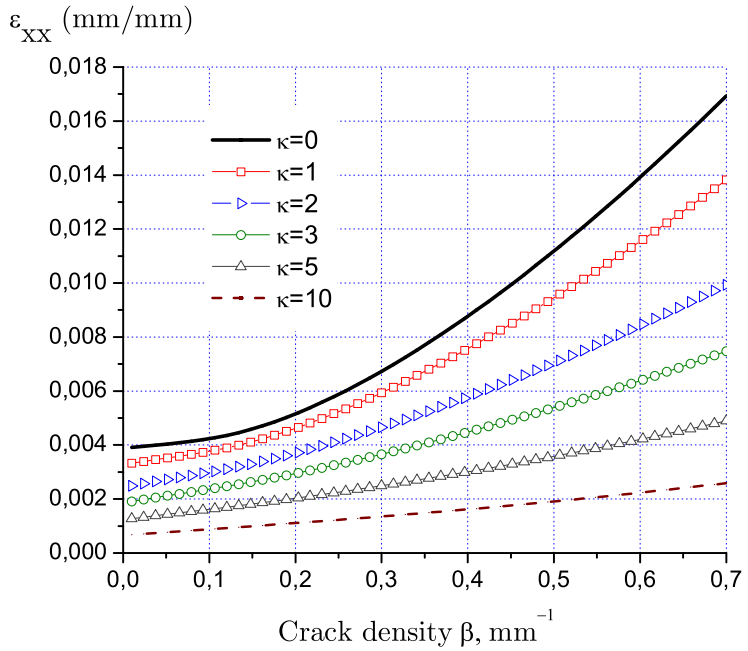

Fig. 5. Relation between applied strain (ε_{xx} and κ) and density of matrix cracks.

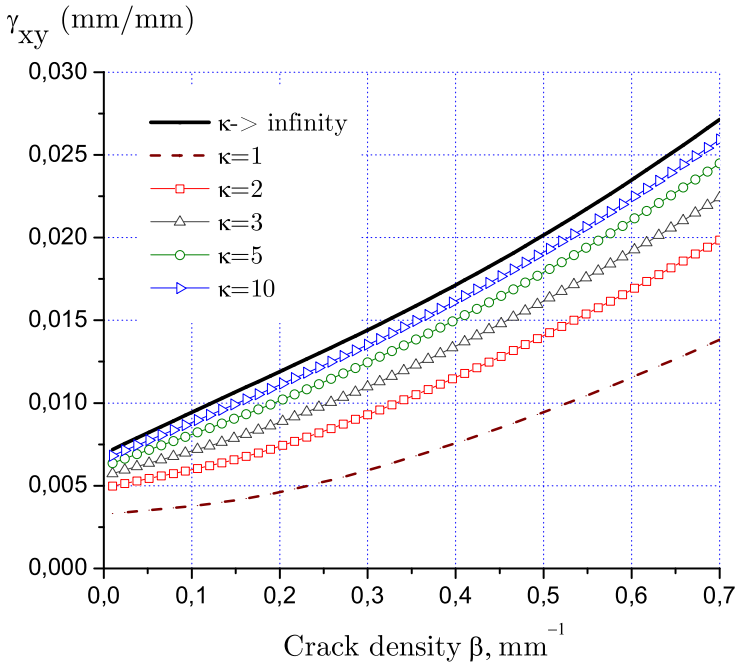

Fig. 6. Relation between applied strain (γ_{xy} and κ) and density of matrix cracks.

The effects of multiaxial strain states on the crack density are clearly shown in Figures 5 and 6. It can be observed in Figure 5 that the density of transverse matrix cracks increases with the multiaxial strain ratio for a fixed value of ε_{xx}.

2.3.2 Transverse compression

Transverse matrix cracks created by a combination of transverse compression and in-plane shear close under the effect of the compressive transverse stress. When a crack closes, its faces can transmit normal tractions but shear tractions may cause slippage between the crack faces. Therefore, it can be assumed that transverse matrix cracks only affect the shear stiffness of a laminate.

Following the procedure described in the previous section, the energy released by the sublaminate 1 is:

$$\Delta U = 2\overline{h}Lb\gamma_{xy}^2\left[A_{66}(L) - A_{66}\left(\frac{L}{2}\right)\right] = 2h^{(1)}bG_{\mathrm{IIc}} \tag{42}$$

The relation between the shear strain and the crack density is obtained as:

$$\gamma_{xy} = \sqrt{\frac{h^{(1)} G_{\mathrm{IIc}}}{\overline{h} L \left[A_{66}(L) - A_{66}\left(\frac{L}{2}\right) \right]}} \tag{43}$$

3 Micromechanics-based damage model

3.1 Constitutive model

A damage model able to represent the onset and accumulation of a periodic distribution of transverse matrix cracks should yield a compliance tensor similar to the one obtained from the micromechanical model, equation (8). An appropriate damage model can be developed by defining the Gibbs free energy per unit volume, Ψ_G, as:

$$\Psi_G = \frac{1}{2}\sigma : \mathbf{H} : \sigma + \Delta T \alpha : \sigma + \Delta M \beta : \sigma \tag{44}$$

or, in the expanded form, as:

$$\begin{aligned} \Psi_G = & \frac{1}{2}\left[\frac{\sigma_{11}^2}{E_1} + \frac{\sigma_{22}^2}{(1-d_2)\,E_2} + \frac{\sigma_{12}^2}{(1-d_6)\,G_{12}} - \left(\frac{\upsilon_{21}}{E_2} + \frac{\upsilon_{12}}{E_1} \right) \sigma_{11}\sigma_{22} \right] + \\ & + (\alpha_{11}\sigma_{11} + \alpha_{22}\sigma_{22})\,\Delta T + (\beta_{11}\sigma_{11} + \beta_{22}\sigma_{22})\Delta M \end{aligned} \tag{45}$$

where E_1, E_2, υ_{12}, υ_{21} and G_{12} are the in-plane elastic orthotropic properties of a unidirectional lamina. The subscript 1 denotes the longitudinal (fiber) direction and 2 denotes the transverse (matrix) direction. d_2 and d_6 are damage variables associated with transverse matrix cracking. α_{11} and α_{22} are the coefficients of thermal expansion in the longitudinal and transverse directions, respectively. β_{11} and β_{22} are the coefficients of hygroscopic expansion in the longitudinal and transverse directions, respectively. ΔT and ΔM are respectively the changes in temperature and moisture content from the stress-free state.

The proposed model distinguishes between active (d_{2+}) and passive damage (d_{2-}) variables, corresponding to the opening or closure of transverse matrix cracks under load reversal respectively. The determination of the active damage variable can be accounted by the following equation:

$$d_2 = d_{2+}\frac{\langle \sigma_{22} \rangle}{|\sigma_{22}|} + d_{2-}\frac{\langle -\sigma_{22} \rangle}{|\sigma_{22}|} \tag{46}$$

where the McCauley operator $\langle x \rangle$ is defined as $\langle x \rangle := \frac{1}{2}(x + |x|)$.

The damage variables d_2 and d_6 can be related to the density of transverse matrix cracks using the micromechanical model previously described.

The constitutive model is obtained from the derivative of the Gibbs free energy with respect to the stress tensor:

$$\varepsilon = \frac{\partial \Psi_G}{\partial \sigma} = \mathbf{H} : \sigma + \Delta T \alpha + \Delta M \beta \tag{47}$$

where the compliance tensor $\mathbf{H}$ is defined as:

$$\mathbf{H} = \frac{\partial^2 \Psi_G}{\partial \sigma^2} = \begin{bmatrix} \frac{1}{E_1} & -\frac{\upsilon_{21}}{E_2} & 0 \\ -\frac{\upsilon_{12}}{E_1} & \frac{1}{(1-d_2)E_2} & 0 \\ 0 & 0 & \frac{1}{(1-d_6)G_{12}} \end{bmatrix} \tag{48}$$

The compliance tensor is established in terms of the damage variables is similar to the compliance tensor derived in the micromechanical model. It is important to note that the damage variables are applied to the H_{22} and H_{66} components of the compliance matrix because the micromechanical model results indicates that $\upsilon_{21}(\beta)/E_2(\beta) = \upsilon_{21}/E_2$ is independent of damage (Figure 3).

Using the stiffness tensor $\mathbf{C} = \mathbf{H}^{-1}$, it is possible to re-write equation (47) as:

$$\sigma = \mathbf{C} : (\varepsilon - \Delta T \alpha - \Delta M \beta) \tag{49}$$

with:

$$\mathbf{C} = \frac{1}{\Lambda} \begin{bmatrix} E_1 & (1-d_2)E_2\upsilon_{12} & 0 \\ (1-d_2)E_1\upsilon_{21} & (1-d_2)E_2 & 0 \\ 0 & 0 & \Lambda(1-d_6)G_{12} \end{bmatrix} \tag{50}$$

and $\Lambda = 1 - \upsilon_{21}\upsilon_{12}(1-d_2)$.

In the context of Continuum Damage Mechanics it is necessary to relate the effective stress tensor, $\tilde{\sigma}$, used in the damage activation and evolution functions to the the nominal stress tensor σ. The relation between the effective and nominal stress tensors is established in the proposed model using the Principle of Strain Equivalence [34]:

$$\tilde{\sigma} = \mathbf{M} : \sigma \tag{51}$$

where the damage operator, $\mathbf{M}$, can be obtained from equations (48) and (50):

$$\mathbf{M} = \mathbf{C}|_{d_i=0} : \mathbf{H} = \begin{bmatrix} 1 & \dfrac{\upsilon_{12} d_2}{(1-d_2)(1-\upsilon_{21}\upsilon_{12})} & 0 \\ 0 & \dfrac{1-\upsilon_{21}\upsilon_{12}+\upsilon_{21}\upsilon_{12} d_2}{(1-d_2)(1-\upsilon_{21}\upsilon_{12})} & 0 \\ 0 & 0 & \dfrac{1}{1-d_6} \end{bmatrix} \tag{52}$$

Using (8) and (48) the damage variables d_2 and d_6 can be expressed in terms of the crack density β as:

$$d_{2+} = 1 - \frac{1}{E_2 H_{22}(\beta)} \tag{53}$$

$$d_6 = 1 - \frac{1}{G_{12} H_{66}(\beta)} \tag{54}$$

The functions $H_{22}(\beta)$ and $H_{66}(\beta)$ are obtained from equations (9) and (10) with $\beta = 1/(2L)$.

It can be shown that the damage variables are defined between zero, when crack spacing tends to infinity, and one, when the crack spacing tends to zero. The relation between the density of transverse matrix cracks β and the damage variables d_2 and d_6 is shown in Figure 7.

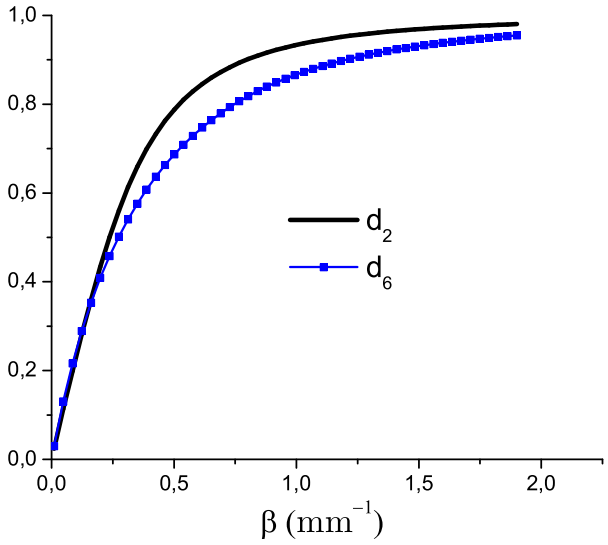

Fig. 7. Relation between the damage variables d_2 and d_6 and density of transverse matrix cracks.

The condition of positive energy dissipation is established as a function of the thermodynamic forces, $\mathbf{Y}$, and as a function of the time derivative of the damage variables, $\dot{\mathbf{d}}$, and it is given by:

$$\Xi = \mathbf{Y} \cdot \dot{\mathbf{d}} = \frac{\partial \Psi_G}{\partial \mathbf{d}} \cdot \dot{\mathbf{d}} \geq 0$$

or

$$\Xi = \frac{\sigma_{22}^2}{2\left(1-d_{2+}\right)^2 E_2}\dot{d}_{2+} + \frac{\sigma_{12}^2}{2\left(1-d_6\right)^2 G_{12}}\dot{d}_6 \geq 0 \tag{55}$$

where Ξ is the rate of energy dissipation per unit volume.

The rate of dissipation can be established in terms of micromechanical variables by using equations (46-54):

$$\frac{1}{\left(1-d_{2+}\right)^2 E_2} = \left[H_{22}\left(\beta\right)\right]^2 E_2 \tag{56}$$

$$\frac{1}{\left(1-d_6\right)^2 G_{12}} = \left[H_{66}\left(\beta\right)\right]^2 G_{12} \tag{57}$$

The time derivatives of the damage variables are:

$$\dot{d}_{2+} = \frac{1}{\left[H_{22}\left(\beta\right)\right]^2 E_2} \frac{\partial H_{22}\left(\beta\right)}{\partial \beta} \dot{\beta} \tag{58}$$

$$\dot{d}_{6} = \frac{1}{\left[H_{66}\left(\beta\right)\right]^2 G_{12}} \frac{\partial H_{66}\left(\beta\right)}{\partial \beta} \dot{\beta} \tag{59}$$

Therefore, the rate of energy dissipated is:

$$\Xi = \frac{\sigma_{22}^2}{2} \frac{\partial H_{22}\left(\beta\right)}{\partial \beta} \dot{\beta} + \frac{\sigma_{12}^2}{2} \frac{\partial H_{66}\left(\beta\right)}{\partial \beta} \dot{\beta} \geq 0 \tag{60}$$

Taking into account that $\frac{\partial H_{22}(\beta)}{\partial \beta} \geq 0$ and $\frac{\partial H_{66}(\beta)}{\partial \beta} \geq 0$, the time derivative of β must be greater than or equal to zero in order to assure positive dissipation, i.e., $\dot{\beta} \geq 0$. Therefore, the condition of positive dissipation, when interpreted from a micromechanical point of view, establishes that the density of transverse matrix cracks can only increase or remain constant.

3.1.1 Damage activation functions

Transverse matrix cracks are predicted using two scalar functions, F_k ($k = 2+, 2-$), established in terms of the effective stress tensor $\tilde{\sigma}^t$, and of the damage threshold value, r^t:

$$F_k := \phi_k \left(\tilde{\sigma}^t\right) - r^t \leq 0 \tag{61}$$

where t is the current time. The initial threshold value, r°, is equal to 1, and the following condition must be satisfied in order to fulfill the Second Principle of Thermodynamics:

$$\dot{r} \geq 0 \tag{62}$$

Damage onset occurs when any of the functions $\phi_k\left(\tilde{\sigma}^t\right)$ reaches the initial damage threshold value of 1. The functions $\phi_k\left(\tilde{\sigma}^t\right)$ used to predict transverse matrix cracking are based on the LaRC04 failure criteria previously proposed by the authors [4,5].

The damage activation functions are used to predict the onset of transverse matrix cracks lying in ply thickness direction, as shown in Figure 1.

Transverse matrix cracks lying in the direction of the ply thickness occur under transverse tension ($\sigma_{22} \geq 0$), or under moderate values of transverse compression and in-plane shear ($\sigma_{22} < 0$).

For high values of transverse compression, the matrix fractures lie along a plane that is inclined at an angle α to the direction of the ply thickness, as shown in Figure 8.

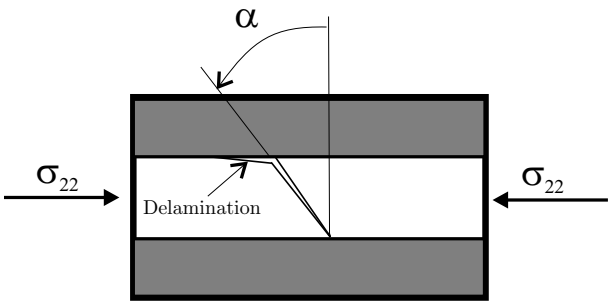

Fig. 8. Matrix crack in a created by high in-plane compressive transverse stress.

Inclined fracture planes caused by transverse compression induce delamination between the plies. This damage mechanism is usually catastrophic in uniformly stressed composites where local redistribution to more lightly loaded regions of the structure cannot occur [6]. Therefore, laminate failure can be assumed to occur when matrix cracking under high values of transverse compression is predicted.

The damage activation function used to predict matrix cracking under transverse tension ($\tilde{\sigma}^t_{22} \geq 0$) and in-plane shear is defined as:

$$F_{2+} := \phi_{2+}\left(\tilde{\sigma}^t\right) - r^t \leq 0 \tag{63}$$

with:

$$\phi_{2+}\left(\tilde{\sigma}^t\right) = \sqrt{(1-g)\,\frac{\tilde{\sigma}^t_{22}}{Y_{\mathrm{T}}} + g\left(\frac{\tilde{\sigma}^t_{22}}{Y_{\mathrm{T}}}\right)^2 + \left(\frac{\tilde{\sigma}^t_{12}}{S_{\mathrm{L}}}\right)^2} \tag{64}$$

The damage activation function used to predict matrix cracking with $\alpha = 0^\circ$ under moderate values of transverse compression ($\tilde{\sigma}^t_{22} < 0$) and in-plane shear is defined as:

$$F_{2-} := \phi_{2-}\left(\tilde{\sigma}^t\right) - r^t \leq 0 \tag{65}$$

with:

$$\phi_{2\text{-}}\left(\tilde{\sigma}^t\right) \underset{\alpha=0^o}{=} \frac{1}{S_L}\left\langle\left|\tilde{\sigma}^t_{12}\right| + \eta^L \tilde{\sigma}^t_{22}\right\rangle \tag{66}$$

The equations proposed can accurately predict transverse matrix transverse cracking. The failure envelope, or initial elastic limit, predicted using equations (63) and (65), and the corresponding experimental data are shown in Figure 9.

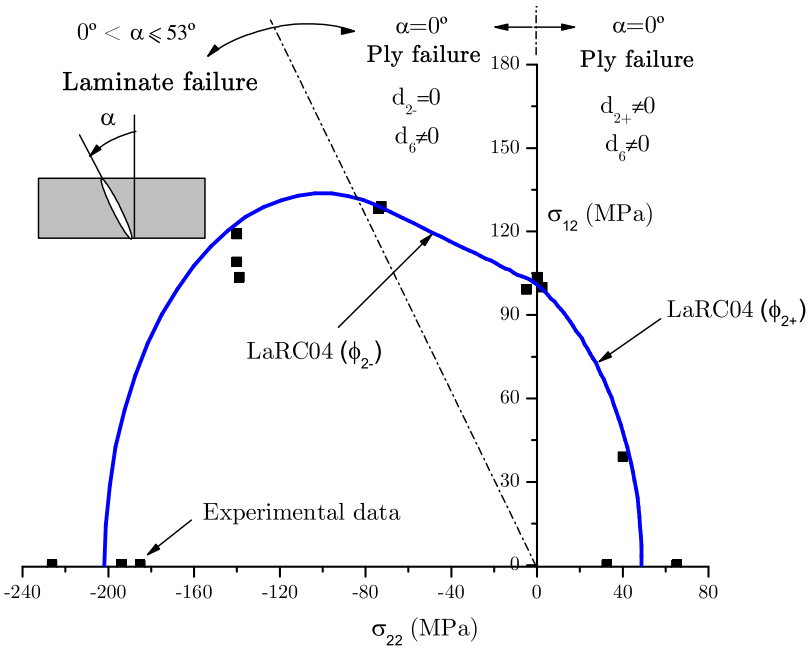

Fig. 9. Comparison between predictions and experimental data [36] and definition of ply or laminate failure domains.

Figure 9 also shows the domain of validity of the model: the damage model is only defined for fracture angles $\alpha = 0°$. For $\alpha > 0°$ the laminate is assumed to fail.

3.1.2 Damage evolution functions

Using the principle of strain equivalence, the effective stress tensor can be written as a function of the strain and undamaged stiffness tensors:

$$\tilde{\sigma} = \mathbf{C}^o \colon \varepsilon \tag{67}$$

The strain tensor is established in terms of the density of transverse cracks and the multiaxial strain ratio κ, equations (27-28). Therefore, all terms in the damage threshold functions can be formulated as a function of the density of transverse matrix cracks and of the the multiaxial strain ratio:

$$F_k = f(\beta^t, \kappa^t) \tag{68}$$

For a given state of strain at time t the multiaxial strain ratio is a dependent variable that can be easily defined using equation (19) in material coordinates:

$$\kappa^t = \frac{\gamma_{12}^t}{\varepsilon_{11}^t} \tag{69}$$

The density of transverse matrix cracks is a state variable. Therefore, it is necessary to define an evolution law subjected to thermodynamic restrictions.

The first condition to be satisfied is the requirement of positive dissipation. As demonstrated by equations (56)-(60), the condition of positive dissipation is satisfied when the evolution of the state variable β is defined by a monotonic increasing function:

$$\dot{\beta} \geq 0 \tag{70}$$

Furthermore, it is necessary to define the conditions for the evolution of the elastic domain:

$$F_k(\tilde{\sigma}^t, \beta^t) \leq 0 \tag{71}$$

$$\dot{\beta} F_k(\tilde{\sigma}^t, \beta^t) = 0 \tag{72}$$

Equations (70)-(72) are the Kuhn-Tucker conditions which ensure a consistent evolution of damage during loading and load reversals.

The evolution laws of the state variables are defined as:

$$\dot{\tilde{\sigma}} = \frac{\partial \tilde{\sigma}}{\partial \varepsilon} : \dot{\varepsilon} = \frac{\partial \tilde{\sigma}}{\partial \varepsilon} : \left(\frac{\partial \varepsilon}{\partial \beta} \dot{\beta} + \frac{\partial \varepsilon}{\partial \kappa} \dot{\kappa} \right) = \mathbf{C}^{o} : \left(\frac{\partial \varepsilon}{\partial \beta} \dot{\beta} + \frac{\partial \varepsilon}{\partial \kappa} \dot{\kappa} \right) \tag{73}$$

$$\dot{r} = \frac{\partial r}{\partial \beta} \dot{\beta} + \frac{\partial r}{\partial \kappa} \dot{\kappa} \tag{74}$$

For a given loading state, the damage consistency condition must be applied to define the evolution of the internal variables. The consistency condition is defined as:

$$F_k = 0 \Rightarrow \dot{F}_k = \frac{\partial F_k}{\partial \tilde{\sigma}} : \dot{\tilde{\sigma}} + \frac{\partial F_k}{\partial r} \dot{r} = 0 \tag{75}$$

From (63) and (65):

$$\frac{\partial F_k}{\partial r} = -1 \tag{76}$$

Using (76) in (75):

$$\dot{F}_k = \frac{\partial F_k}{\partial \tilde{\sigma}} : \dot{\tilde{\sigma}} - \dot{r} = \frac{\partial F_k}{\partial \tilde{\sigma}} : \mathbf{C}^{\mathrm{o}} : \dot{\varepsilon} - \dot{r} = 0 \tag{77}$$

Using equations (73) and (74) in (77):

$$\dot{F}_k = \frac{\partial F_k}{\partial \tilde{\sigma}} : \mathbf{C}^{\mathrm{o}} : \left(\frac{\partial \varepsilon}{\partial \beta} \dot{\beta} + \frac{\partial \varepsilon}{\partial \kappa} \dot{\kappa} \right) - \left(\frac{\partial r}{\partial \beta} \dot{\beta} + \frac{\partial r}{\partial \kappa} \dot{\kappa} \right) = 0 \tag{78}$$

Taking into account that the micromechanical model proposed assumes a constant loading ratio, $\dot{\kappa} = 0$:

$$\dot{F}_k = \frac{\partial F_k}{\partial \tilde{\sigma}} : \left(\mathbf{C}^{\mathrm{o}} : \frac{\partial \varepsilon}{\partial \beta} - \frac{\partial r}{\partial \beta} \right) \dot{\beta} = 0 \tag{79}$$

The density of of transverse matrix cracks, β, is calculated from the integration of equation (79) using a numerical method, such as the return-mapping algorithm.

For damage evolution under transverse tension, the values of $\partial F_k / \partial \tilde{\sigma}$ can be obtained from (63):

$$\frac{\partial F_{2+}}{\partial \tilde{\sigma}_{11}} = 0 \tag{80}$$

$$\frac{\partial F_{2+}}{\partial \tilde{\sigma}_{22}} = \frac{1}{\phi_{2+}} \left(\frac{1-g}{2} \frac{1}{Y_{\mathrm{T}}} + g \frac{\tilde{\sigma}_{22}}{(Y_{\mathrm{T}})^2} \right) \tag{81}$$

$$\frac{\partial F_{2+}}{\partial \tilde{\sigma}_{12}} = \frac{1}{\phi_{2+}} \frac{\tilde{\sigma}_{12}}{(S_{\mathrm{L}})^2} \tag{82}$$

and for damage evolution under transverse compression (65):

$$\frac{\partial F_{2-}}{\partial \tilde{\sigma}_{11}} = 0 \tag{83}$$

$$\frac{\partial F_{2-}}{\partial \tilde{\sigma}_{22}} = \frac{\eta^L}{S_{\mathrm{L}}} \tag{84}$$

$$\frac{\partial F_{2-}}{\partial \tilde{\sigma}_{12}} = \left\{ \begin{array}{l} \frac{1}{S_L} \tilde{\sigma}_{12} \text{ if } \tilde{\sigma}_{12} \geq 0 \\ \frac{-1}{S_L} \tilde{\sigma}_{12} \text{ if } \tilde{\sigma}_{12} < 0 \end{array} \right\} = \frac{1}{S_{\mathrm{L}}} |\tilde{\sigma}_{12}| \tag{85}$$

Figure 10 represents the evolution of the elastic domain for different values of the crack density β using a ply with the material properties shown in Table 1.

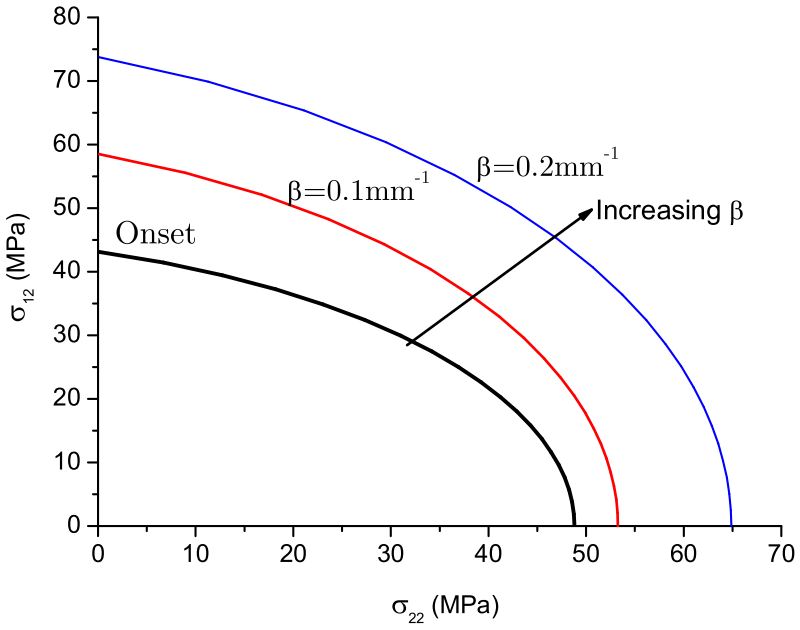

Fig. 10. Predicted evolution of the elastic domain as a function of crack density β.

4 Prediction of laminate failure

In the presence of stress concentrations the onset of fiber localized failure does not cause immediate structural collapse. Experimental results [37,38] have shown that structural collapse is caused by the the progression of fiber fracture. Therefore, it is necessary to use a damage model that accounts for the stress re-distributions caused by fiber fractures.

The model proposed here assumes that for uniformly stressed laminates the onset of fiber fracture and delamination caused by high compressive transverse stresses triggers structural collapse. Therefore, laminate final failure is predicted when fiber failure or matrix cracking with $\alpha \neq 0^\circ$ occurs.

4.1 Fiber failure

The criterion for fiber fracture under longitudinal tension ($\sigma_{11} \geq 0$) is defined as [4,5]:

$$\mathrm{FI}_{1+} := \frac{\sigma_{11}}{X_\mathrm{T}} - 1 \leq 0 \tag{86}$$

where X_T is the ply tensile strength in the longitudinal direction.

The LaRC03 failure criterion for fiber kinking under longitudinal compression ($\sigma_{11} < 0$) is a function of the components of the stress tensor in a frame representing the fiber misalignment, $\sigma_{ij}^{(m)}$ [4,5]:

$$\begin{aligned}
\sigma_{11}^{(m)} &= \sigma_{11}\cos^2\varphi + \sigma_{22}\sin^2\varphi + 2\,|\sigma_{12}|\sin\varphi\cos\varphi \\
\sigma_{22}^{(m)} &= \sigma_{11}\sin^2\varphi + \sigma_{22}\cos^2\varphi - 2\,|\sigma_{12}|\sin\varphi\cos\varphi \\
\sigma_{12}^{(m)} &= -\sigma_{11}\sin\varphi\cos\varphi + \sigma_{22}\sin\varphi\cos\varphi + |\sigma_{12}|\left(\cos^2\varphi - \sin^2\varphi\right)
\end{aligned} \tag{87}$$

where the fiber misalignment angle φ is defined as [4]:

$$\varphi = \frac{|\sigma_{12}| + (G_{12} - X_\mathrm{C})\,\varphi^c}{G_{12} + \sigma_{11} - \sigma_{22}} \tag{88}$$

where

$$\varphi^c = \tan^{-1}\left[\frac{1-\sqrt{1-4\left(\frac{S_{\mathrm{L}}}{X_{\mathrm{C}}}+\eta^L\right)\left(\frac{S_{\mathrm{L}}}{X_{\mathrm{C}}}\right)}}{2\left(\frac{S_{\mathrm{L}}}{X_{\mathrm{C}}}+\eta^L\right)}\right] \tag{89}$$

and where X_{C} is the ply compressive strength in the longitudinal direction.

Depending on the sign of the in-plane transverse stress $\sigma_{22}^{(m)}$, the criteria for fiber kinking ($\sigma_{11} < 0$) are:

$$\mathrm{FI}_{1\text{-}} := \left\langle \frac{\left|\sigma_{12}^{(m)}\right| + \eta^L \sigma_{22}^{(m)}}{S_{\mathrm{L}}} \right\rangle - 1 \leq 0,\ \sigma_{22}^{(m)} < 0 \tag{90}$$

or

$$\mathrm{FI}_{1\text{-}} := (1-g)\,\frac{\sigma_{12}^{(m)}}{Y_{\mathrm{T}}} + g\left(\frac{\sigma_{12}^{(m)}}{Y_{\mathrm{T}}}\right)^2 + \left(\frac{\sigma_{12}^{(m)}}{S_{\mathrm{L}}}\right)^2 - 1 \leq 0,\ \sigma_{22}^{(m)} \geq 0 \tag{91}$$

4.2 Matrix failure with $\alpha \neq 0^\circ$

The failure criteria for matrix cracking under transverse compression ($\sigma_{22} < 0$) and in-plane shear and $\alpha \neq 0^\circ$ are defined as [4,5]:

$$\mathrm{FI}_{2\text{-}} := \left(\frac{\tau_e^T}{\mathrm{S_T}}\right)^2 + \left(\frac{\tau_e^L}{\mathrm{S_L}}\right)^2 - 1 \leq 0, \sigma_{11} \geq -\mathrm{Y_C} \tag{92}$$

$$\mathrm{FI}_{2\text{-}} := \left(\frac{\tau_e^{(m)T}}{\mathrm{S_T}}\right)^2 + \left(\frac{\tau_e^{(m)L}}{\mathrm{S_L}}\right)^2 - 1 \leq 0, \sigma_{11} < -\mathrm{Y_C} \tag{93}$$

where the effective shear stresses in the fracture plane are defined as:

$$\begin{aligned} \tau_e^T &= \left\langle \left|\tau^T\right| + \eta^T \sigma_n \cos\theta \right\rangle \\ \tau_e^L &= \left\langle \left|\tau^L\right| + \eta^L \sigma_n \sin\theta \right\rangle \end{aligned} \tag{94}$$

where $\theta = \tan^{-1}\left(\frac{-|\sigma_{12}|}{\sigma_{22}\sin\alpha}\right)$. The components of the stress tensor on the fracture plane are given by [4,5]:

$$\begin{cases} \sigma_n = \sigma_{22} \cos^2 \alpha \\ \tau^T = -\sigma_{22} \sin \alpha \cos \alpha \\ \tau^L = \sigma_{12} \cos \alpha \end{cases} \tag{95}$$

The terms τ_e^{mT} and τ_e^{mL} are calculated from equations (94)-(95) using the relevant components of the stress tensor established in a frame representing the fiber misalignment, equation (87). The angle α is determined by maximizing the failure index FI_{2-} (92-93) using a simple iterative procedure.

The coefficients of transverse and longitudinal influence, η^T and η^L respectively, are [4,5]:

$$\eta^T = \frac{-1}{\tan 2\alpha_0} \tag{96}$$

$$\eta^L = -\frac{\mathrm{S_L} \cos 2\alpha_0}{\mathrm{Y_C} \cos^2 \alpha_0} \tag{97}$$

with $\alpha_0 \approx 53^\circ$. Y_C is the ply compressive strength in the transverse direction.

5 Examples

The present damage model can be used in combination with classical lamination theory using stand-alone codes. Alternatively, the damage model can be implemented as a constitutive subroutine for the Finite Element Method.

The damage model was implemented using a commercial symbolic computing software. The model was verified by calculating the response of several glass-epoxy laminates under uniaxial and multiaxial loads: $[\pm 45/90_4]_s$, $[0_2/90_4]_s$, $[0_2/90_2]_s$ and $[0_2/90]_s$.

In all calculations performed, the ply thickness was taken as 0.144mm and the temperature difference from the stress free condition -100°C. The coefficients of thermal expansion in the longitudinal and transverse directions are $\alpha_{11} = 7.43 \times 10^{-6}/^\circ\mathrm{C}$ and $\alpha_{22} = 22.4 \times 10^{-6}/^\circ\mathrm{C}$, respectively. The remaining material properties used are shown in Tables 2 and 3.

Table 2
Elastic properties of glass-epoxy [20]

E_1 (GPa)	E_2 (GPa)	G_{12} (GPa)	G_{23} (GPa)	υ_{12}	υ_{23}	χ (10^{-8}MPa^{-3})
44.7	12.8	5.8	4.5	0.30	0.42	2.0

Table 3
Strengths and fracture toughnesses of glass-epoxy [20].

Y_T^{ud} (MPa)	S_L^{ud} (MPa)	G_{Ic} (N/mm^{-1})	G_{IIc} (N/mm^{-1})
40.0	73.0	0.20	0.40

The predicted response of $[\pm 40/90_4]_s$ and $[0_2/90_4]_s$, is shown in Figure 11 for two values of the multiaxial strain ratio: $\kappa = 0$ and $\kappa = 10$.

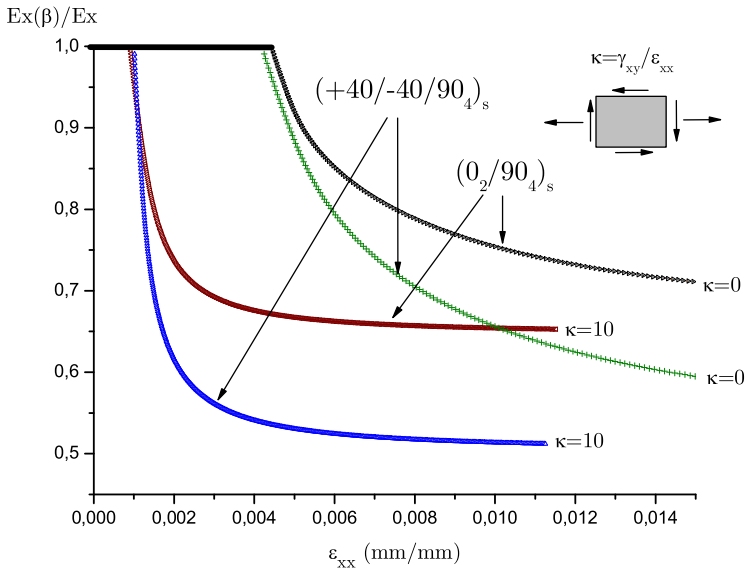

Fig. 11. Relation between laminate modulus and applied strain for $[\pm 45/90_4]_s$ and $[0_2/90_4]_s$ laminates.

Figure 11 shows that the rate of degradation of the elastic properties of the laminate is higher when the axial stiffness of the outer sublaminate decreases. The effect of multiaxial loading is also clear in Figure 11: as expected, the application of shear strains leads to a reduction of the extension corresponding to the onset of transverse matrix cracks and to a higher rate of degradation of the elastic properties of the laminate.

Figure 12 compares the response of $[0_2/90_4]_s$, $[0_2/90_2]_s$ and $[0_2/90]_s$ laminates for $\kappa = 0$ and $\kappa = 2$.

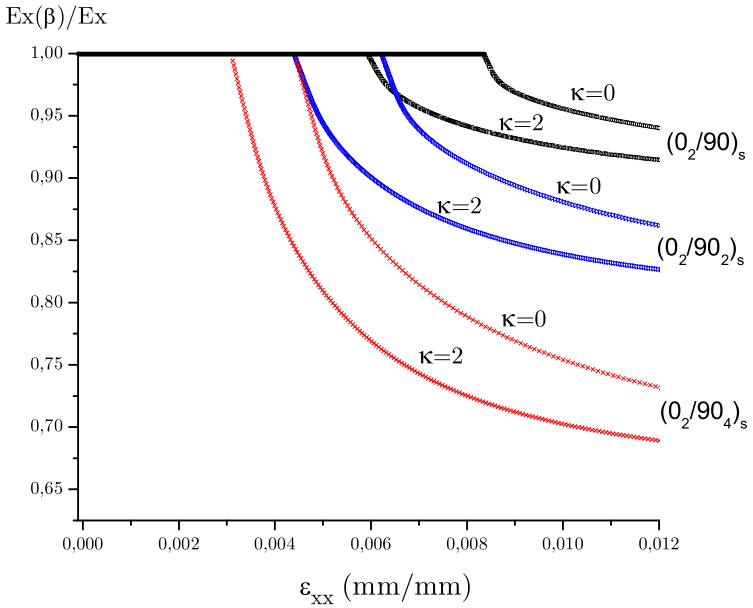

Fig. 12. Relation between laminate modulus and applied strain for $[0_2/90_4]_s$, $[0_2/90_2]_s$ and $[0_2/90]_s$ laminates.

The in-situ effect is shown in Figure 12. For $\kappa = 0$, the strain corresponding to the onset of matrix cracking of the $[0_2/90]_s$ laminate is 1.9 and 1.3 times higher than the ones of the $[0_2/90_4]_s$ and $[0_2/90_2]_s$ laminates respectively. Furthermore, the strain at the onset of matrix cracking of the $[0_2/90]_s$ is 2.7 times higher than the ultimate transverse strain measured in an unidirectional test specimen.

The laminate modulus calculated using the proposed model and the ply discount method is shown in Figure 13 for a $[0_2/90_4]_s$ laminate. The ply discount method assumes that $E_2 \approx 0$ and $G_{12} \approx 0$ as soon as the failure criterion is satisfied.

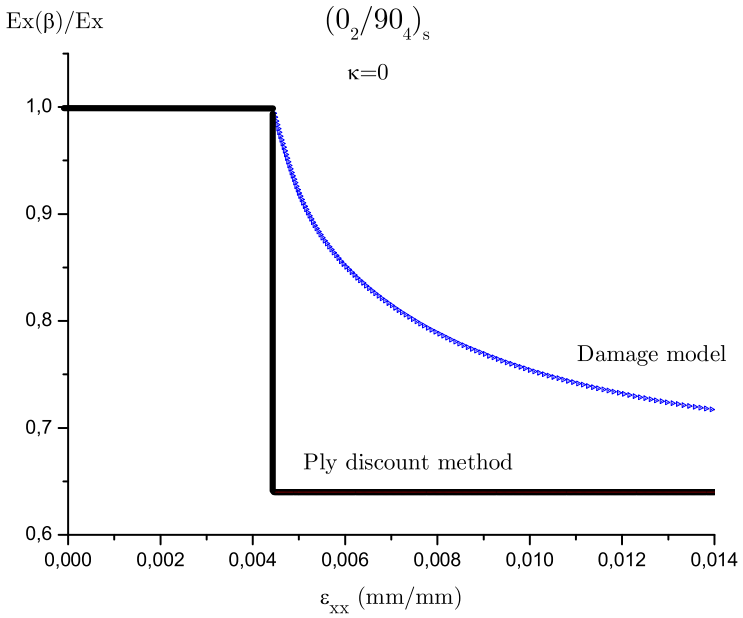

Fig. 13. Laminate modulus calculated using the damage model and the ply-discount method.

It can be observed in Figure 13 that the response of the modulus of the laminate obtained using the ply-discount method is a step-function that does not accurately represent the progressive degradation of the laminate.

6 Conclusions

A new, micromechanics-based, continuum damage model able to simulate the onset and propagation of transverse matrix cracks and final laminate failure is proposed. The model is applicable to $[\pm\theta/90_n]_s$ laminates, under multiaxial loading and uniform stresses or small stress gradients.

The model uses ply properties and does not require any tests performed at laminate level to identify damage onset and evolution functions. The onset of damage is predicted using failure criteria and damage evolution laws are established from the micromechanical analysis of cracked plies.

The model can be used in Finite Element analysis, and the results are independent of the mesh refinement because the constitutive model does not result in strain-softening. The onset and accumulation of transverse matrix cracks are represented as a distributed damage mechanism. The onset of localization, which is triggered by either fiber fracture or matrix cracking with $\alpha \neq 0$, is assumed to cause a structural collapse.

The predictions show that the rate of degradation of the elastic properties increases when the stiffness of the outer sublaminate decreases. Decreasing the thickness of the 90° plies also increases the degradation rate.

Acknowledgements

The authors would like to thank Professor Janis Varna, Luleå University of Technology, Sweden, for the useful discussions.

The present work has been partially funded by the Spanish Government under research project MAT2003-09768-C03-001.

The financial support of the Portuguese Foundation for Science and Technology (FCT) under the project PDCTE/EME/50354/2003 is acknowledged by the second author.

References

[1] MIL-HDBK-17-3F, Military Handbook, Polymer Matrix Composites. U.S. Department of Defense, 2002.

[2] Hinton, M. J.; Kaddour, A. S., and Soden, P. D. A comparison of the predictive capabilities of current failure theories for composite laminates, judged against experimental evidence. Composites Science and Technology. 2002; 62:1725-1797.

[3] Soden, P. D.; Kaddour, A. S., and Hinton, M. J. Recommendations for designers and researchers resulting from the worl-wide failure exercise. Composites Science and Technology. 2004; 64:589-604.

[4] Dávila, C. G and Camanho, P. P. Failure criteria for FRP laminates in plane stress. NASA/TM-2003-212663. National Aeronautics and Space Administration; 2003.

[5] Pinho, S. T.; Dávila, C. G.; Camanho, P. P.; Iannucci, L., and Robinson, P. Failure models and criteria for FRP under in-plane shear or three-dimensional stress states including shear non-linearity. NASA/TM-2005-213530. National Aeronautics and Space Administration; 2005.

[6] Puck, A. and Schürmann, H. Failure analysis of FRP laminates by means of physically based phenomenological models. Composites Science and Technology. 1998; 58:1045-1067.

[7] Liu, K. S and Tsai, S. W. A progressive quadratic failure criterion for a laminate. Composites Science and Technology. 1998; 58:1023-1032.

[8] Bažant, Z. P. Size effect. International Journal of Solids and Structures. 2000; 37:69-80.

[9] Ladevèze, P. On a damage mechanics approach. Mechanics and Mechanisms of damage in composites and multi-materials. D. Batiste ed. London: ESIS11; 1991; pp. 119-141.

[10] Williams, K. V.; Vaziri, R., and Poursartip, A. A physically based continuum damage mechanics model for thin laminated composite structures. International Journal of Solids and Structures. 2003; 40:2267-2300.

[11] Varna, J.; Joffe, R.; Akshantala, N. V., and Talreja, R. Damage in composite laminates with off-axis plies. Composites Science and Technology. 1999; 59:2139-2147.

[12] Allen, D. H.; Harris, C. E., and Groves, S. E. A thermomechanical constitutive theory for elastic composites with distributed damage- I. theoretical development. International Journal of Solids and Structures. 1987; 23(9):1301-1318.

[13] Allen, D. H.; Harris, C. E., and Groves, S. E. A thermomechanical constitutive theory for elastic composites with distributed damage- II. application to

matrix cracking in laminated composites. International Journal of Solids and Structures. 1987; 23(9):1319-1338.

[14] Herakovich, C. T. Mechanics of Fibrous Composites. Wiley, 1997.

[15] Bažant, Z. P. and Oh, B. H. Crack band theory for fracture of concrete. Matériaux Et Constructions. 1983; 16(93):155-177.

[16] Jirásek, M. Modeling of localized damage and fracture in quasibrittle materials. Lecture Notes in Physics 568, ed. P.A. Vermeer et al. 2001; pp. 17-29.

[17] Nuismer, R. J. and Tan, S. C. Constitutive Relations of a Cracked Composite Lamina. Journal of Composite Materials. 1988; 22:306-321.

[18] Tan, S. C. and Nuismer, R. J. A Theory for Progressive Matrix Cracking in Composite Laminates. Journal of Composite Materials. 1989; 23:1029-1047.

[19] Berglund, L. A.; Varna, J., and Yuan, J. Effect of intralaminar toughness on the transverse cracking strain in cross-ply laminates. Advanced Composite Materials. 1991; 1(3):225-234.

[20] Joffe, R.; Krasnikovs, A., and Varna, J. COD-based simulation of transverse cracking and stiffness reduction in (S/90n)s laminates . Composites Science and Technology. 2001; 61:637-656.

[21] Joffe, R. and Varna, J. Analytical modeling of stiffness reduction in symmetric and balanced laminates due to cracks in 90 layers. Composites Science and Technology. 1999; 59:1641-1652.

[22] Varna, J.; Joffe, R., and Talreja, R. A synergistic damage-mechanics analysis of transverse cracking in $(\pm\theta/90_4)$s laminates. Composites Science and Technology. 2001; 61:657-665.

[23] Dvorak, G. J.; Laws, N., and Hejazi, M. Analysis of progressive matrix cracking in composite laminates I. thermoelastic properties of a ply with cracks. Journal of Composite Materials. 1985; 19:216-234.

[24] Laws, N.; Dvorak, G. J., and Hejazi, M. Stiffness changes in unidirectional composites caused by crack systems. Mechanics of Materials. 1983; 2:123-137.

[25] Nguyen, B. N. A three-dimensional modeling of transverse matrix cracking in laminated composites. Key Engineering Materials. 1997; 127-131:1117-1126.

[26] Schoeppner, G. A. and Pagano, N. J. 3-D thermoelastic moduli and saturation crack density for cross-ply laminates with transverse cracks. International Journal of Damage Mechanics. 1999; 8:1-37.

[27] Hashin, Z. Analysis of cracked laminates: a variational approach. Mechanics of Materials. 1985; 4:121-136.

[28] Highsmith, A. L. and Reifsnider, K. L. Stiffness-reduction mechanisms in composite laminates. Damage in Composite Materials. American Society for Testing and Materials; 1982; pp. 103-117.

[29] Hashin, Z. Analysis of stiffness reduction of cracked cross-ply laminates. Engineering Fracture Mechanics. 1986; 25(5/6):771-778.

[30] McCartney, L. N.; Schoeppner, G. A., and Becker, W. Comparison of models for transverse ply cracks in composite laminates. Composites Science and Technology. 2000; 60:2347-2359.

[31] Camanho, P. P.; Dávila, C. G.; Pinho, S. T.; Iannucci, L., and Robinson, P. Prediction of in situ strengths and transverse matrix cracking in composites under transverse tension and in-plane shear. Composites-Part A. 2006; 37:165-176.

[32] Dvorak, G. J. and Laws, N. Analysis of first ply failure in composite laminates. Engineering Fracture Mechanics. 1986; 25(5/6):763-770.

[33] Hahn, H. T. A mixed-mode fracture criterion for composite materials. Composites Technology Review. 1983; 5:26-29.

[34] Lemaitre, J. A Course on Damage Mechanics. Springer, 1996.

[35] Soden, P. D.; Hinton, M. J., and Kaddour, A. S. Lamina properties, lay-up configurations and loading conditions for a range of fibre-reinforced composite laminates. Composites Science and Technology. 1998; 58:1011-1022.

[36] Swanson, S. R. A micro-mechanical model for in-situ compression strength of fiber composite laminates, Transactions of the American Society of Mechanical Engineers, Series H, Journal of Engineering Materials and Technology. 1992; 114:8-12.

[37] Camanho, P. P.; Bowron, S., and Matthews, F. L. Failure mechanisms in bolted CFRP. Journal of Reinforced Plastics and Composites. 1998; 17:205-233.

[38] Camanho, P. P. Application of numerical methods to the strength prediction of mechanically fastened joints in composite laminates. PhD Thesis, Centre for Composite Materials, Department of Aeronautics, Imperial College London, U.K.; 1999.

[39] Maple 8 Users Manual. Waterloo Maple Inc., Canada, 1981.

Appendix A: Laminate constitutive model

The plane stress constitutive equation of a laminate is:

$$\varepsilon = \bar{\mathbf{Q}}^{-\mathbf{1}}\bar{\sigma} \tag{A-1}$$

where the barred parameters denote a quantity that is not a function of the thickness coordinate.

The laminate stiffness $\bar{\mathbf{Q}}$ matrix can be obtained from the stiffness and thickness of the individual plies applying the classical in-plane laminate theory:

$$\bar{\mathbf{Q}} = \frac{1}{\bar{h}}\sum_{k=1}^{n} h^{(k)}\bar{\mathbf{Q}}^{(k)} \tag{A-2}$$

where $\bar{h}$ is the total laminate thickness, $h^{(k)}$ are the thickness of the k^{th} ply and $\bar{\mathbf{Q}}^{(k)}$ is the stiffness of the each k^{th} ply in global laminate coordinate system (see Figure 1)

For a balanced symmetrical laminate the matrix $\bar{\mathbf{Q}}$ is defined as:

$$\bar{\mathbf{Q}} = \begin{bmatrix} \bar{Q}_{11} & \bar{Q}_{12} & 0 \\ \bar{Q}_{21} & \bar{Q}_{22} & 0 \\ 0 & 0 & \bar{Q}_{66} \end{bmatrix} \tag{A-3}$$

The stiffness of a laminate composed by two sublaminates is obtained as:

$$\bar{\mathbf{Q}} = \frac{1}{2\bar{h}}\left(2h^{(1)}\bar{\mathbf{Q}}^{(1)} + 2h^{(2)}\bar{\mathbf{Q}}^{(2)}\right) = \frac{1}{\bar{h}}\left(h^{(1)}\bar{\mathbf{Q}}^{(1)} + h^{(2)}\bar{\mathbf{Q}}^{(2)}\right) \tag{A-4}$$

For a balanced, symmetric laminate, the laminate stiffness depends on the distance between two consecutive longitudinal cracks (L):

$$\bar{\mathbf{A}}(L) = \begin{bmatrix} \bar{A}(L)_{11} & \bar{A}(L)_{12} & 0 \\ \bar{A}(L)_{21} & \bar{A}(L)_{22} & 0 \\ 0 & 0 & \bar{A}(l)_{66} \end{bmatrix} \tag{A-5}$$

where $\bar{A}_{ij}(L), i, j = 1, 2$ are the average laminate stiffness:

$$\bar{A}_{11}(L) = \frac{h^{(1)}Q_{11}^{(1)} + h^{(2)}Q_{11}^{(2)}}{\beta_2 \bar{h}} \tag{A-6}$$

$$\bar{A}_{12}(L) = \frac{\beta_1 h^{(1)}Q_{12}^{(1)} + \beta_2 h^{(2)}Q_{12}^{(2)}}{\beta_2 \bar{h}} \tag{A-7}$$

$$\bar{A}_{22}(L) = \frac{h^{(1)}Q_{22}^{(1)} + h^{(2)}Q_{22}^{(2)}}{\bar{h}} - \left(\frac{\beta_2 - \beta_1}{\beta_2}\right) \frac{h^{(1)}\left(Q_{12}^{(1)}\right)^2}{\bar{h}Q_{11}^{(1)}} \tag{A-8}$$

$\bar{A}_{66}(L)$ is the laminate shear stiffness calculated as:

$$\bar{A}_{66}(l) = \frac{h^{(1)}Q_{66}^{(1)} + h^{(2)}Q_{66}^{(2)}}{\beta_4 \bar{h}} \tag{A-9}$$

The superscript (1) and (2) denote ply 1 and ply 2 respectively and $Q_{ij}^{(k)}, i, j = 1, 2, 6$ are the undamaged lamina stiffness along the laminate axes.

The parameters β_1 and β_2 can be calculated as [18]:

$$\beta_1 = 1 - \frac{\tanh \alpha_1 L}{\alpha_1 L} \tag{A-10}$$

$$\beta_2 = 1 + \left(\frac{h^{(1)}Q_{11}^{(1)}}{h^{(2)}Q_{11}^{(2)}}\right) \frac{\tanh \alpha_1 L}{\alpha_1 L} \tag{A-11}$$

with α_1:

$$(\alpha_1)^2 = \frac{3C_{55}^{(1)}C_{55}^{(2)}}{h^{(1)}C_{55}^{(1)} + h^{(2)}C_{55}^{(2)}} \left(\frac{h^{(1)}Q_{11}^{(1)} + h^{(2)}Q_{11}^{(2)}}{h^{(1)}h^{(2)}Q_{11}^{(1)}Q_{11}^{(2)}}\right) \tag{A-12}$$

where $C_{55}^{(k)}$ is the lamina stiffness in the lamina axes.

The parameter β_4 is be calculated as:

$$\beta_4 = 1 + \left(\frac{h^{(1)}Q_{66}^{(1)}}{h^{(2)}Q_{66}^{(2)}}\right) \frac{\tanh \alpha_2 L}{\alpha_2 L} \tag{A-13}$$

with α_2:

$$(\alpha_2)^2 = \frac{3C_{44}^{(1)}C_{44}^{(2)}}{h^{(1)}C_{44}^{(1)} + h^{(2)}C_{44}^{(2)}} \left(\frac{h^{(1)}Q_{66}^{(1)} + h^{(2)}Q_{66}^{(2)}}{h^{(1)}h^{(2)}Q_{66}^{(1)}Q_{66}^{(2)}} \right) \tag{A-14}$$

where $C_{44}^{(k)}$ is the lamina stiffness in the lamina axes.

The relation between the longitudinal modulus E_x, the Poisson ratio υ_{xy} and the shear modulus G_{xy} and the crack density is obtained $\bar{A}_{ij}(L), i, j = 1, 2, 6$.

After the definition of $\bar{A}_{ij}(L), i, j = 1, 2, 6$ it is possible to calculate the engineering constants of the laminate. The longitudinal modulus, $E_x(L)$, of the quarter cell under plane stress is:

$$\bar{E}_x(L) = \bar{A}_{11}(L) - \frac{\left[\bar{A}_{12}(L)\right]^2}{\bar{A}_{22}(L)} \tag{A-15}$$

The Poisson ration of the laminate is:

$$\bar{\upsilon}_{xy}(L) = \frac{\bar{A}_{12}(L)}{\bar{A}_{22}(L)} \tag{A-16}$$

The shear stiffness of the laminate, $\bar{G}_{xy}(L)$, is obtained as:

$$\bar{G}_{xy}(L) = \bar{A}_{66}(L) \tag{A-17}$$

REPORT DOCUMENTATION PAGE

Form Approved
OMB No. 0704-0188

1. REPORT DATE *(DD-MM-YYYY)*	2. REPORT TYPE	3. DATES COVERED *(From - To)*
21-03-2006	Technical Memorandum	

4. TITLE AND SUBTITLE

A Micromechanics-Based Damage Model for [±Ø/90n]s Composite Laminates

5a. CONTRACT NUMBER

5b. GRANT NUMBER

5c. PROGRAM ELEMENT NUMBER

6. AUTHOR(S)

Joan-Andreu Mayugo; Pedro P. Camanho; Pere Maimí; Carlos G. Dávila

5d. PROJECT NUMBER

5e. TASK NUMBER

5f. WORK UNIT NUMBER

7. PERFORMING ORGANIZATION NAME(S) AND ADDRESS(ES)

NASA Langley Research Center
Hampton, VA 23681-2199

8. PERFORMING ORGANIZATION REPORT NUMBER

L-19242

9. SPONSORING/MONITORING AGENCY NAME(S) AND ADDRESS(ES)

National Aeronautics and Space Administration
Washington, DC 20546-0001

10. SPONSORING/MONITOR'S ACRONYM(S)

NASA

11. SPONSORING/MONITORING REPORT NUMBER

NASA/TM-2006-214285

12. DISTRIBUTION/AVAILABILITY STATEMENT

Unclassified - Unlimited
Subject Category 39
Availability: NASA CASI (301) 621-0390

13. SUPPLEMENTARY NOTES

Mayugo and Maimí: University of Girona; Camanho: University of Porto; Dávila: Langley Research Center

14. ABSTRACT

A new damage model based on a micromechanical analysis of cracked [±Ø/90n]s laminates subjected to multiaxial loads is proposed. The model predicts the onset and accumulation of transverse matrix cracks in uniformly stressed laminates, the effect of matrix cracks on the stiffness of the laminate, as well as the ultimate failure of the laminate. The model also accounts for the effect of the ply thickness on the ply strength. Predictions relating the elastic properties of several laminates and multiaxial loads are presented.

15. SUBJECT TERMS

Fracture Mechanics; Continuum Damage Mechanics; Failure Criteria; Composite Materials.

16. SECURITY CLASSIFICATION OF:			17. LIMITATION OF ABSTRACT	18. NUMBER OF PAGES	19a. NAME OF RESPONSIBLE PERSON
a. REPORT	b. ABSTRACT	c. THIS PAGE			STI Help Desk (email: help@sti.nasa.gov)
U	U	U	UU	43	19b. TELEPHONE NUMBER *(Include area code)* (301) 621-0390